⌘ Author's Choice

© 2012 by The American Society for Biochemistry and Molecular Biology, Inc.
This paper is available on line at http://www.mcponline.org

# Mapping of *O*-GlcNAc Sites of 20 S Proteasome Subunits and Hsp90 by a Novel Biotin-Cystamine Tag*[S]

**Thorsten Overath‡§, Ulrike Kuckelkorn‡, Petra Henklein‡, Britta Strehl‡, David Bonar‡¶, Alexander Kloss‡, Dagmar Siele‡‖, Peter-Michael Kloetzel‡**, and Katharina Janek‡**

**The post-translational modification of proteins with *O*-GlcNAc is involved in various cellular processes including signal transduction, transcription, translation, and nuclear transport. This transient protein modification enables cells or tissues to adapt to nutrient conditions or stress. *O*-Glycosylation of the 26 S proteasome ATPase subunit Rpt2 is known to influence the stability of proteins by reducing their proteasome-dependent degradation. In contrast, knowledge of the sites of *O*-GlcNAcylation on the subunits of the catalytic core of the 26 S proteasome, the 20 S proteasome, and the impact on proteasome activity is very limited. This is predominantly because *O*-GlcNAc modifications are often substoichiometric and because 20 S proteasomes represent a complex protein mixture of different subtypes. Therefore, identification of *O*-GlcNAcylation sites on proteasome subunits essentially requires effective enrichment strategies. Here we describe an adapted $\beta$-elimination-based derivatization method of *O*-GlcNAc peptides using a novel biotin-cystamine tag. The specificity of the reaction was increased by differential isotopic labeling with either "light" biotin-cystamine or deuterated "heavy" biotin-cystamine. The enriched peptides were analyzed by LC-MALDI-TOF/TOF-MS and relatively quantified. The method was optimized using bovine $\alpha$-crystallin and then applied to murine 20 S proteasomes isolated from spleen and brain and murine Hsp90 isolated from liver. Using this approach, we identified five novel and one known *O*-GlcNAc sites within the murine 20 S proteasome core complex that are located on five different subunits and in addition two novel *O*-GlcNAc sites on murine Hsp90$\beta$, of which one corresponds to a previously described phosphorylation site.** ***Molecular & Cellular Proteomics 11: 10.1074/mcp.M111.015966, 467–477, 2012.***

From the ‡Institut für Biochemie, Charité-Universitätsmedizin Berlin, 13347 Berlin, Germany, the §Institut für Experimentelle Medizin, AG Systematische Proteomforschung, Christian-Albrechts-Universität, 24105 Kiel, Germany, the ¶Institut für Biochemie II, Universität Köln, 50931 Köln, Germany, and ‖GE Healthcare, 80807 München, Germany

Received November 18, 2011, and in revised form, March 30, 2012
Published, MCP Papers in Press, May 3, 2012, DOI 10.1074/mcp.M111.015966
⌘ *Author's Choice*—Final version full access.

The ubiquitin proteasome system is the major ATP-dependent protein degradation machinery of eukaryotic cells (1). It plays an essential role in cell cycle, differentiation, apoptosis, regulation of transcription, adaptation to stress, and immune surveillance (2–4). The central catalytic part of the ubiquitin proteasome system, the 20 S proteasome, is composed of seven different $\alpha$- and $\beta$-subunits each, which are organized in four stacked heptameric rings ($\alpha_{1-7}$, $\beta_{1-7}$, $\beta_{1-7}$, and $\alpha_{1-7}$). The two $\alpha$-rings connect the attachment of regulatory complexes like the 19 S particle or the proteasome activator PA28 forming the 26 S proteasome and hybrid proteasomes, respectively, whereas the two inner $\beta$-rings carry the catalytic subunits $\beta$1, $\beta$2, and $\beta$5. Upon immunological challenge and stress, *i.e.*, oxidative and heat stress, genes encoding the three alternative catalytic subunits ($\beta$1i, $\beta$2i, and $\beta$5i) are expressed leading to the formation of immunoproteasomes with altered proteolytic characteristics, thereby improving the capacity of the proteasome (3, 5). Alternatively, eukaryotic cells can adapt proteasome activity to changing environmental conditions by post-translational modifications of proteasome subunits (6–9). Distinct proteasome subunits were found to be phosphorylated (10–12), acetylated (13–16), or *O*- GlcNAcylated (17–19). A regulatory role of *O*-linked glycosylation in proteasome function was supported by the finding that modification of the 19 S regulator complex subunit Rpt2 inhibited the proteolytic activity of 26 S proteasomes and resulted in substrate protein stabilization (18, 20). Recently, inhibition of an *O*-GlcNAcase isoform was shown to modulate the ubiquitin proteasome system, which further supports the functional importance of *O*-GlcNAc modification of proteasomes (21).

The monomeric *O*-GlcNAc[1] modification occurs on hydroxyl groups of serine or threonine residues of nuclear and cytoplasmic proteins. In several cases *O*-GlcNAcylation takes place at the same or adjacent to the sites of phosphorylation. Growing evidence suggests an extensive cross-talk between

[1] The abbreviations used are: *O*-GlcNAc, *O*-linked $\beta$-*N*-acetylglucosamine; OGT, *O*-GlcNAc transferase; OGA, *O*-GlcNAcase; BiCy, biotin-cystamine; EDC, 1-ethyl-3-[3-dimethylaminopropyl] carbodiimide hydrochloride; Fmoc, *N*-(9-fluorenyl)methoxycarbonyl; L, light; H, heavy.

both modifications, indicating a regulatory role in cellular signaling (22). Dysregulations of the *O*-GlcNAc cycling enzymes *O*-GlcNAc transferase (OGT) and *O*-GlcNAcase (OGA) are associated with malignancy, diabetes mellitus, and neurodegenerative diseases (9, 23).

The dynamic nature and low stoichiometry of *O*-GlcNAc modifications (which is particular true for 20 S proteasomes) represents a major analytical challenge. Therefore, the mapping of *O*-GlcNAc sites by mass spectrometry requires effective enrichment strategies. Previously, a number of methods have been applied to solve this problem, including wheat germ agglutinin enrichment (24), chemical derivatization (25) and chemoenzymatic labeling coupled with affinity or titanium dioxide chromatography (26–28), periodate oxidation, and hydrazide resin capture (29). However, despite these analytical developments within the last years, only one *O*-GlcNAc site on human erythrocyte proteasomes ($\alpha$5 subunit) has been identified so far (19).

Here, we describe an adapted derivatization method that included $\beta$-elimination followed by Michael addition with dithiothreitol (25, 30) of *O*-GlcNAc peptides using a novel biotin-cystamine tag to identify *O*-GlcNAc sites on 20 S proteasome and Hsp90. Because phosphorylated and nonmodified serine and threonine residues also react via the $\beta$-elimination/Michael addition mechanism, the specificity of the reaction was increased by differential isotopic labeling with either "light" biotin-cystamine (BiCy-d0) or deuterated "heavy" biotin-cystamine (BiCy-d4). The enriched peptides were analyzed by LC-MALDI-TOF/TOF-MS and relatively quantified.

## EXPERIMENTAL PROCEDURES

*Chemicals*—Sequencing grade trypsin and alkaline shrimp phosphatase were obtained from Promega GmbH (Mannheim, Germany). The $\alpha$-*O*-GalNAc peptide was synthesized by Biosynthan GmbH (Berlin, Germany). Protein A-Sepharose was obtained from GE Healthcare. Dulbecco's modified Eagle's medium was obtained from Biochrom AG (Berlin, Germany). The antibody CTD 110.6, OGA (jack bean), $\alpha$-crystallin, and all other chemicals were obtained from Sigma. The MALDI matrix $\alpha$-cyano-4-hydroxycinnamic acid (Sigma-Aldrich) was recrystallized.

*Synthesis and Purification of Model Peptides*—The *O*-GlcNAc peptide AIPVgSREEKPSSAPSS-COOH (with exception of the glycosylated serine) and phosphorylated analogs of the eight identified *O*-GlcNAc peptides of 20 S proteasomes and Hsp90 (GpSSAGFDR-COOH; RPFGlpSAL-COOH; SpSLIILK-COOH, LVpSLIGSK, LpSEGFSIH-COOH; DVFlpSAAER-COOH; FYEAFpSK-COOH; and LpSELLR-COOH) were synthesized on an ABI peptide synthesizer 433A with standard Fmoc methods.

For the *O*-GlcNAc peptide, the manual coupling of 1.2–1.5 eq. of Fmoc-Ser($\beta$-D-GlcNAc(Ac)$_3$)-OH (IRIS Biotech GmbH, Marktredwitz, Germany) was performed with *N*,*N*-diisopropyl-carbodiimide/1-hydroxy-7-Azabenzotriazole (1:1:1) in dimethylformamid for 24 h. After coupling, the resin was acetylated, and synthesis was continued at the peptide synthesizer. The cleavage of the three protection acetyl groups of the sugar was executed with 6% (v/v) $H_2O_2$ in absolute methanol for 6 h.

For the synthesis of phosphopeptides, *N*-$\alpha$-Fmoc-*O*-benzyl-L-phosphoserine (Merck/Novabiochem) was used. All of the peptides were cleaved from the resin by treatment with 92:5:3 (v/v) TFA/water/triisopropylsilane, precipitated with diethyl ether, and lyophilized. Peptide purification was carried out by using preparative HPLC, and peptide identity was confirmed by MALDI-MS.

*Synthesis of the Biotin-cystamine-d0/d4 Tag*—The synthesis of the biotin-cystamine tag was performed in three steps: (i) protection of free thiol groups of cystamine by formation of disulfide bonds, (ii) condensation of cystamine with biotin, and (iii) reduction of disulfide bridges between cystamine residues. 100 mg of cystamine-d0 (Sigma) or cystamine-d4 (CDN Isotopes) were dissolved in 200 ml of 0.1 M $NaHCO_3$ (pH 8). For disulfide bond formation 2 ml of 0.3% (v/v) $H_2O_2$ were added, and the solution was stirred for 45 min at room temperature. The completeness of the reaction was monitored with Ellman's reagent and stopped by the addition of 10% (v/v) acetic acid in water. The reaction mixture was lyophilized. The condensation of the biotin moiety with the disulfide was performed by adding 3 eq of biotin and 3 eq of EDC/hydroxybenzotriazole. EDC and the disulfide were dissolved in 5 ml of $H_2O$, biotin, and hydroxybenzotriazole in 10 ml of DMSO, respectively, and both mixtures were combined. The solution was stirred at 40 °C for 3 h. The resulting precipitate was filtered and washed with DMSO/dimethylformamide. Afterward the solution was lyophilized. The crude product was dissolved in dimethylformamide and purified by HPLC on a Shimadzu LC-8A system with a Kromasil column (100–10-C18, 50 × 250 mm) at a flow rate of 50 ml/min. Mobile phase (A) was 0.2% TFA in water and (B) 0.2% TFA in 80:20 (v/v) acetonitrile/water. The gradient was performed from 15 to 45% B in 60 min. 25 mg of the purified condensation product was dissolved in 30:70 (v/v) acetonitrile/water and reduced by Tris (2-carboxyethyl)phosphine hydrochloride at pH 5. The reduced biotin-cystamine-d0 or biotin-cystamine-d4 was purified on a Gemini C18 column (250-mm × 21.2-mm inner diameter, 10 $\mu$m; Phenomenex) at a flow rate of 20 ml/min with a water-acetonitrile gradient from 19 to 44% B in 50 min. The purified BiCy-d0/d4 was lyophilized and stored at 4 °C until further use.

*20 S Proteasome and Hsp90 Purification*—Spleen, liver, and brain tissues from 15 mice (C57BL/6) were pooled, and proteasomes were isolated (with PUGNAC) according to a standard procedure (31, 32) (Hsp90, which often co-purifies with 20 S proteasome from liver, was separated in the last purification step by hydrophobic interaction chromatography with phenyl-Superose; $(NH_4)_2SO_4$ was added to the 20 S proteasome and Hsp90 containing sample to a final concentration of 1.2 M. The proteins were applied onto a phenyl-Superose column (PC1.6/5, gel volume 1.7 ml; GE Healthcare) and eluted by a linear decreasing ammonium sulfate gradient (20 ml) from 1.2 to 0 M $(NH_4)_2SO_4$. The purity of the separated proteasomes and of Hsp90 was controlled by SDS-PAGE, and protein concentrations were calculated according the Bradford protocol (Bio-Rad).

*Western Blot*—The proteins were separated by 15% SDS-PAGE and blotted onto a PVDF membrane, and Western blotting was performed according to standard protocols (32). Immunodetection using the monoclonal mouse *O*-GlcNAc antibody CTD 110.6 followed the manufacturer's instructions. For detection of the proteasome, the rabbit antisera MP1 (anti-20 S proteasome) or K378 (anti-$\alpha$4 subunit; both lab stocks) were used. Hsp90 was detected by a monoclonal Hsp90 antibody (Enzo Life Sciences, UK).

*Immunoprecipitation*—Four $\mu$l of antibody CTD110.6 or 2 $\mu$l of proteasome antibodies, *i.e.* K378 and K08, were added to the clarified cell lysate, incubated overnight at 4 °C and precipitated by anti-IgM or protein A-Sepharose, respectively. The bound proteins were detached by hot SDS sample buffer. SDS-PAGE and Western blotting were performed as described. For detection of the primary antibody, a protein A-POD conjugate was used (Bio-Rad).

*Labeling of Proteasomes with [$^{14}$C]Glucosamine*—RMA cells were washed in PBS and resuspended in Dulbecco's modified Eagle's

medium without glucose, 10% FCS, 1% penicillin/streptomycin, 50 $\mu$M $\beta$-mercaptoethanol, and 2 mM glutamine to obtain $5 \times 10^6$ cells/ml. Two ml of the cell suspension were incubated with 10 $\mu$Ci of [$^{14}$C]glucosamine/ml for 1, 2, and 3 h at 37 °C. The cells were washed twice with ice-cold PBS and lysed with 0.5% Nonidet P-40 in PBS. Proteasomes were precipitated with proteasome antibody K08 (lab stock) and protein A-Sepharose overnight, followed by intensive washing of the Sepharose. The proteins were desorbed by boiling the protein A-Sepharose in SDS sample buffer and then separated by SDS-PAGE under standard conditions. The acrylamide gel was dried, and the labeled proteins were detected by autoradiography.

*Performic Acid Oxidation*—Prior to oxidation the samples (10 $\mu$g of $\alpha$-crystallin, 100 $\mu$g of Hsp90, or 300 $\mu$g of 20 S proteasomes) were precipitated with methanol/chloroform according to the protocol of the ClickiT® *O*-GlcNAc enzymatic labeling kit (Invitrogen). The dried protein pellets were oxidized with performic acid vapor in an exsiccator containing 1 ml of performic acid (5:95 (v/v) 30% $H_2O_2$/85% formic acid) for 2 h at room temperature (33).

*Tryptic Digestion*—The oxidized protein pellets were resuspended in 100 $\mu$l of 50 mM ammonium bicarbonate in 5:95 (v/v) acetonitrile/water. Tryptic digestion was performed for 16–18 h at 37 °C and stopped with 10 $\mu$l of 10% (v/v) TFA in water, and samples were dried in a vacuum centrifuge.

*Deglycosylation and Dephosphorylation*—Dried peptides were dissolved in 20 $\mu$l of *O*-GlcNAcase buffer (20 mM sodium citrate in water, pH 6) and incubated for 10 min at 99 °C to inactivate remaining active trypsin. Afterward the internal standard peptides $\beta$-*O*-GlcNAc (AIPVS($\beta$-*O*-GlcNAc)REEKPSSAPSS, 20 pmol, 1 $\mu$l) and $\alpha$-*O*-GalNAc (FVFDRPLPVS($\alpha$-*O*-GalNAc)R, 80 pmol, 1 $\mu$l) were added. The $\beta$-*O*-GlcNAc-modified peptide was only used for the 20 S proteasome and Hsp90 preparations because its amino acid sequence originates from the tryptic peptide 158–173 of bovine $\alpha$-crystallin chain A. The peptide mixture was split in equal halves. One half was deglycosylated first with 0.1 unit of OGA for 16 h and then with 0.1 unit for 3 h at 37 °C. Equal volume of *O*-GlcNAcase buffer without *O*-GlcNAcase was added to the untreated sample (final volume, 30 $\mu$l). Dephosphorylation of both samples was performed with 5 units of shrimp alkaline phosphatase for 3 h at 37 °C. The concentration of the phosphatase buffer in the final 90-$\mu$l volume was 50 mM Tris-HCl, 0.5 mM $MgCl_2$ in $H_2O$ (pH 9).

*Chemical Derivatization with BiCy-d0/d4*—The glycosylated sample (without OGA, with shrimp alkaline phosphatase) was derivatized with BiCy-d0 and the deglycosylated sample (with OGA, with shrimp alkaline phosphatase) with BiCy-d4 (vice versa in label switch experiments). Therefore, 90 $\mu$l of double concentrated $\beta$-elimination/Michael addition solution (0.4% (w/v) NaOH, 4% (v/v) triethylamine) containing 10 mM BiCy-d0 or BiCy-d4 were added to the samples (final pH 11.5). The samples were incubated for 2 h at 52 °C. The reaction was stopped by adjusting the pH of the solutions to pH 7 with 20% (v/v) TFA.

*Chemical Derivatization of Model Peptides*—10 pmol of the $\beta$-*O*-GlcNAc, $\alpha$-*O*-GalNAc, or phosphorylated model peptides were dissolved in 50 $\mu$l of 0.2% (w/v) NaOH, 2% (v/v) triethylamine containing 5 mM BiCy-d0 or BiCy-d4 and incubated for 2 h at 52 °C in a thermomixer. The reaction was stopped by adding 5 $\mu$l of 20% (v/v) TFA (pH $<$ 4), and the samples were C18-$\mu$ZipTip (Millipore) desalted prior to MS analysis.

*Enrichment of BiCy-d0/d4 Peptides*—BiCy-d0- and BiCy-d4-labeled samples were combined, and excess of BiCy derivatization reagent was removed by size exclusion chromatography on a Superdex peptide 3.2/30 column (3.2 $\times$ 300 mm) (GE Healthcare) using a SMART fast protein liquid chromatography system (Amersham Biosciences) at a flow rate of 60 $\mu$l/min water. The peptide containing fractions (UV absorption at 214 nm) were lyophilized and solved in 100 $\mu$l of streptavidin binding solution (0.02% (w/v) BSA, 0.2 M NaCl, 50 mM Tris-HCl in $H_2O$, pH 7.5). BiCy-d0/d4-labeled peptides were purified with 100 $\mu$l of magnetic streptavidin beads (Dynabeads MyONE™ Streptavidin T1; Invitrogen). The loading and washing procedures (with avoidance of detergents) were performed with slight modifications as described by Girault *et al.* (34). Briefly, before use, the beads were washed with 0.1% BSA in 50 mM Tris-HCl, pH 7.4 (solution A), after 30 min of sample incubation 100 $\mu$l of water was added for 30 min. Then the supernatant was removed, and the beads were extensive washed with solution A, solution B (0.1% BSA in 50 mM Tris-HCl, pH 7.4, 1 M NaCl), and water. Saturation of streptavidin sites was performed with biotin. After final washing with water, the biotinylated peptides were eluted from the resin by 2 $\times$ 50 $\mu$l of 70:30 (v/v) acetonitrile/water, 0.1% (v/v) TFA (adapted from Girault *et al.* (34)), and the eluent was dried in a vacuum centrifuge.

*LC-MALDI-TOF/TOF-MS/MS*—LC-MS/MS analyses were performed on a 4700 proteomics Analyzer (Applied Biosystems, Framingham, MS) off-line coupled with an Ultimate HPLC system and Probot fractionation device (Dionex, Idstein, Germany). Dried peptides were resuspended in 12 $\mu$l of 0.1% (v/v) TFA in water. Ten $\mu$l of the sample were concentrated on a trap column (PepMap C18, 5 $\mu$m, 5-mm $\times$ 300-$\mu$m inner diameter; Dionex). LC separations were performed on an analytical column (PepMap C18, 3 $\mu$m, 150 mm $\times$ 75 $\mu$m; Dionex) at a flow rate of 200 nl/min. Mobile phase (A) was 2:98 (v/v) acetonitrile/water containing 0.05% (v/v) TFA and (B) was 80:20 (v/v) acetonitrile/water containing 0.045% (v/v) TFA. Gradients were 0–15% B in 4 min and 15–60% B in 40 min for $\alpha$-crystallin, in 60 min for Hsp90 and in 100 min for 20 S proteasomes. Column effluent was continuously mixed with MALDI matrix (5 mg/ml $\alpha$-cyano-4-hydroxycinnamic acid in 70:30 (v/v) acetonitrile/water containing 0.1% (v/v) TFA, 1 $\mu$l/min) and spotted at 10-s intervals on 26 $\times$ 12 spot arrays on MALDI steel targets (Applied Biosystems). Mass spectra were acquired in a data-dependent mode. The MS spectra were recorded in the mass range of *m/z* 700–4000 and with the accumulation of 2000 subspectra. MS/MS spectra were measured from the five most intensive precursor ions (S/N $>$ 30). 5000–10,000 laser shots were accumulated. Known contaminations such as matrix peaks and sodium adducts as wells as signals $\pm$ 4 Da from an already fragmented precursor (because of the 4 Da difference of BiCy-d0/d4 tag) were excluded from fragmentation.

*Data Processing and Relative Quantification*—MS and MS/MS peaklists were generated by the "Peak to Mascot" tool of the 4000er Series Explorer v 3.6. For MS/MS data analysis, MASCOT server (version 2.2; Matrixscience, London, UK) was used to search in-house against Swissprot FASTA database (www.uniprot.org; build date February 15, 2012; 525,207 sequences). 20 S proteasome and Hsp90 samples were searched with the taxonomy filter *Mus musculus* activated (sequences after taxonomy filter 16.345). $\alpha$-Crystallin samples were searched against a small FASTA file containing only two Swissprot entries for bovine $\alpha$-crystallin chain A and B. As parameters were set, enzyme: trypsin with a maximum of two missed cleavages or semitrypsin; mass tolerances: 100 ppm for precursor and 0.2 Da for MS/MS fragment ions; variable modifications: BiCy-d0/d4 of Ser (372,144/376,144), Thr (386,160/390,160), or Cys (372,144/376,144) oxidation of Met and His (+15,994, +31,999) or of Cys and Trp (+15,994, +31,999, +47,982) and N-terminal Gln to pyro-Glu (−17,027). −17,027). MS/MS spectra of identified peptides (ionscore $>$15 and peptide rank 1) were verified by manual inspection of their fragmentation pattern. The identity of specific BiCy-labeled peptides of 20 S proteasomes and Hsp90 was confirmed by comparison of their MS/MS spectra with synthetic BiCy-d0-labeled analogs.

Relative quantification of BiCy-d0/d4-labeled ion pairs was performed manually by adding the intensities of the monoisotopic peaks according to their LC elution profile (3–7 spectra) and calculating the

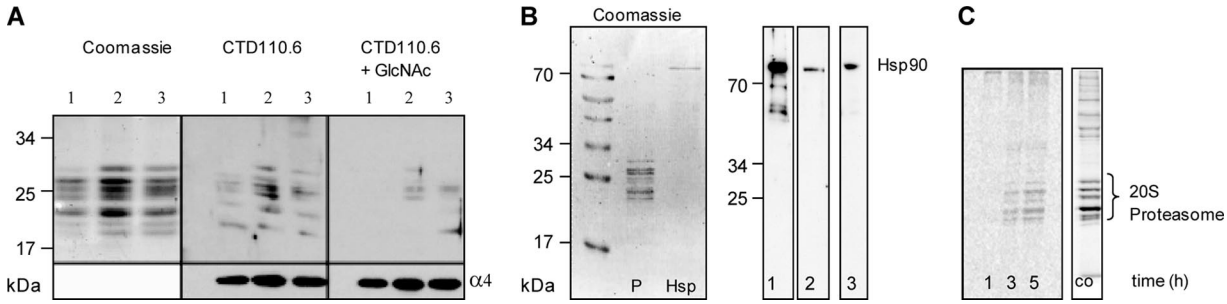


FIG. 1. **Detection of *O*-GlcNAcylation on proteasomes and Hsp90.** *A*, detection of *O*-GlcNAc-modifications on diverse mouse tissue proteasomes with the *O*-GlcNAc antibody CTD110.6. Proteasomes were isolated from mouse liver (1), mouse spleen (2), and mouse brain (3). Three $\mu$g of each were separated by SDS-PAGE. The *left panel* shows the staining with Coomassie, the *middle panel* shows the detection of *O*-GlcNAc modifications with CTD110.6, and the *right panel* shows the competition of CTD110.6 with 500 mM GlcNAc. Proteasome subunit $\alpha$4 was detected as loading control. *B*, detection of *O*-glycosylation on murine Hsp90. Co-purified Hsp90 was isolated from proteasomes, and both were separated by SDS-PAGE. The Coomassie staining of proteasomes (*lane P*), and Hsp90 is shown in the *left panel*. Hsp90 can be detected with CTD 110.6 (*right panel*, *lane 1*). The signal is diminished by saturation of the antibody with 500 mM GlcNAc (*lane 2*). The detection of Hsp90 with a monoclonal Hsp90 antibody is shown in *lane 3*. *C*, *in vivo* labeling of proteasomes with [$^{14}$C]glucosamine. RMA cells (murine) were incubated with [$^{14}$C]glucosamine for 1, 3, and 5 h. As control (*lane co*), [$^{35}$S]Met-labeled 20 S proteasomes were used. The labeled proteasomes were precipitated with the polyclonal proteasome antibody K08. The precipitated protein was analyzed in SDS-PAGE and detected by autoradiography.

ratios of BiCy-d0/BiCy-d4 peptides (L/H ratio), as well of BiCy-d4/BiCy-d0 peptides (H/L ratio) in the label switch experiment, respectively. The L/H ratio (H/L) of the $\alpha$-*O*-GalNAc standard peptide was used to calculate a normalization factor, which was applied to all observed L/H ratios (or H/L ratios) of identified peptides to compensate inevitable fluctuations during sample preparation.

## RESULTS

To study 20 S proteasomes modified with *O*-GlcNAc, 20 S proteasomes were isolated from murine tissues. *O*-GlcNAcylation was detected in Western blots using the monoclonal antibodies CTD110.6 (Fig. 1*A*) and MAI-076, as well as the ClickiT® system (data not shown). Proteasomes derived from liver, spleen, and brain were positively stained for *O*-linked glycosylation. In addition, co-purified Hsp90 separated from liver proteasomes was also shown to be *O*-GlcNAc-modified (Fig. 1*B*). To verify the glycosylation of 20 S proteasomes, murine RMA cells were incubated in presence of [$^{14}$C]glucosamine. Within 3–5 h of incubation, multiple proteasomal subunits were labeled with [$^{14}$C]glucosamine, *i.e.*, modified with *O*-GlcNAc (Fig. 1*C*). Remarkably, in all experiments, several of the 17 different proteasomal subunits were shown to be *O*-GlcNAc-modified.

Zhang *et al.* (18) proposed a tight connection between glucose metabolism and proteasome activity. However, the influence of glucose metabolism on glycosylation and the activity of the catalytic proteasome core complex remained unstudied. To analyze the impact of glycosylation on 20 S proteasomes, murine fibroblast cells were cultured with glucose at a physiological concentration of 5 mM, as well as with 10 mM.

When cells were pulsed with 10 mM glucose for 240 min, we observed a transient reduction of the proteasome activity within the first 60 min (Fig. 2*A*), corroborating earlier results of Zhang *et al.* (18). However, comparing the initial activity (0 min) with those after 240 min, a slight increase in proteasomal peptide hydrolyzing activity was observed. Furthermore, an incubation of cells with a high glucose concentration of 10 mM was accompanied by an *O*-glycosylation of 20S proteasome subunits (Fig. 2*B*). The change in glycosylation of proteasomal subunits was also demonstrated by immunoprecipitation of *O*-GlcNAc-modified proteasomes with the antibody CTD110.6 and the detection of *O*-GlcNAcylation in immunoprecipitated proteasomes (supplemental Fig. 1). The proteasome modification with *O*-GlcNAc was significantly enhanced upon increased glucose concentration in the culture medium.

*Derivatization of O-GlcNAc Peptides with a Biotin-cystamine Tag*—Based on above data, we set out to identify the sites of *O*-GlcNAc modification on 20 S proteasome subunits. For chemical modification of *O*-GlcNAc peptides by alkali-mediated $\beta$-elimination and Michael addition, initial experiments were performed with the tag dithiothreitol as described by Wells *et al.* (25) and Vosseller *et al.* (30). Although the derivatization and thiol-Sepharose enrichment of samples with low complexity ($\beta$-*O*-GlcNAc model peptide and $\alpha$-crystallin) allowed the detection of the expected *O*-GlcNAc sites, for the analysis of complex 20 S proteasomes the procedure was unsatisfactory (data not shown). Because of the often observed extremely low stoichiometry of the *O*-GlcNAc modification on proteins, it is essential that the tag allows an efficient affinity purification of the labeled peptides. Therefore, we synthesized a new tag with a biotin moiety (Fig. 3*A*), which allows the usage of streptavidin instead of thiol-Sepharose. The thiol group of the cystamine moiety of the tag imparts the *S*-nucleophilic attack of $\beta$-eliminated serine and threonine residues. It is known, however, that the $\beta$-elimination/Michael addition reaction is not only specific for *O*-GlcNAc-modified serine and threonine residues. Unspecific de-

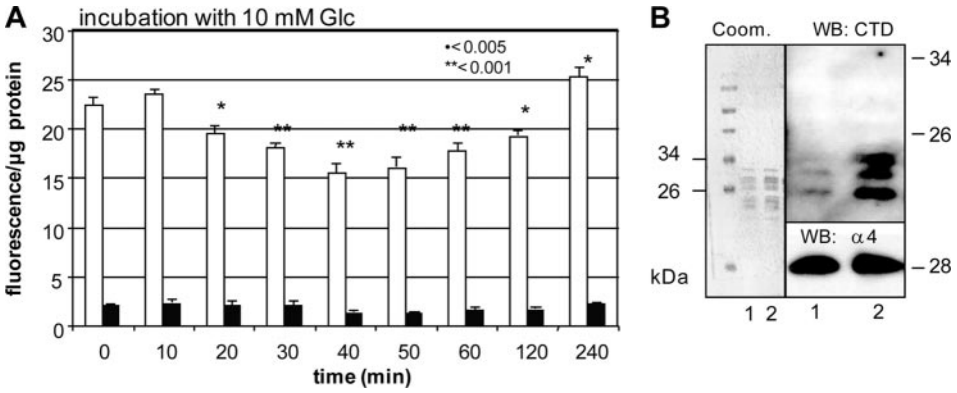


FIG. 2. **Glucose concentration in culture medium influences proteasome activity and proteasome glycosylation.** *A*, murine fibroblast cells (line C4) were incubated with 10 mM glucose in the culture medium for indicated time points in a 24-well plate. The cells were washed and lysed with 0.1% Nonidet P-40 in 20 mM Tris buffer, pH 7.2. The proteolytic activity within the lysates was monitored by hydrolysis of suc-LLVY-AMC (*white bars*). In parallel, the proteasome activity was inhibited by 10 $\mu$M MG132 (*black bars*). *B*, proteasomes were isolated from the C4 mouse fibroblast cell line cultured with 5 mM (*lane 1*) and 10 mM (*lane 2*) glucose for 2 h. In the *left panel* Coomassie staining of the separated proteasomes is shown, and in the *right panel* the detection of *O*-GlcNAc modifications by CTD110.6 is shown. Immunodetection of proteasome subunit $\alpha$4 served as loading control. *WB*, Western blot.

rivatization of cysteine, alkylated cysteine, serine, and threonine residues that are unmodified or phosphorylated can occur (25, 30, 33, 35). To discriminate between specific derivatization of *O*-GlcNAc sites and unspecific modified residues, we synthesized a "light" BiCy-d0 and a deuterated "heavy" BiCy-d4 tag that allow relative quantification. Fig. 3*B* shows the MS spectra of the synthetic *O*-GlcNAc-modified peptide AIPVgSREEKPSSAPSS, which corresponds to the C-terminal, tryptic peptide 158–173 of bovine $\alpha$-crystallin chain A before and after derivatization with BiCy-d0. The tagging results in a mass shift of *m/z* +82 compared with the *O*-GlcNAc-modified peptide. Under MS/MS conditions the tag generates indicator ions that are diagnostic for the presence of BiCy-derivatized peptides and therefore allow a sensitive screening for modified peptides. The signal at *m/z* 304.1 corresponds to the protonated BiCy-d0, at *m/z* 227.1 to the biotinylium ion (36) and the neutral loss of 303 mass units at *m/z* 1624.8 to the fragment $[M\text{-BiCy-d0}+H]^+$ (Fig. 3*C*). The *O*-GlcNAc site can be localized to $Ser^5$ because of the difference of 372 mass units between the y11 and y12 ion corresponding to the BiCy-d0 serine residue.

*Enrichment and Relative Quantification of BiCy-tagged O-GlcNAcylated Peptides*—To avoid unspecific tagging of cysteine residues, the proteins were first oxidized by performic acid and then proteolytically digested (Fig. 4). The samples were split in halves and treated first with or without OGA and then with phosphatase. After enzyme incubation, the samples were derivatized with equivalent amounts of BiCy-d0 or BiCy-d4 and then combined. Excess of free BiCy tag was removed by size exclusion chromatography, followed by enrichment of BiCy-tagged peptides by affinity chromatography on streptavidin (supplemental Fig. 2) and LC-MS/MS analysis including relative quantification. In principle, the specificity of the procedure could be also changed to the analysis of phosphorylation sites, when the split samples are treated with or without phosphatase and with OGA as performed by Vosseller *et al.* (30).

As internal controls for the relative quantification, the $\beta$-*O*-GlcNAc peptide AIPVS($\beta$-*O*-GlcNAc)REEKPSSAPSS and the $\alpha$-*O*-GalNAc peptide FVFDRPLPVS($\alpha$-*O*-GalNAc)R were spiked to the samples. The *O*-$\beta$-GlcNAc peptide was used to prove the degylcosylation efficiency. The L/H ratio for this internal standard peptide was always greater than 10. Because $\alpha$-*O*-glycosidic bonds cannot be cleaved by OGA, the $\alpha$-*O*-GalNAc peptide was used to mimic an unspecific derivatization with an L/H ratio of about 1 (supplemental Fig. 3).

*Enrichment of BiCy-tagged Peptides from $\alpha$-Crystallin*—The experimental approach was first tested with the standard *O*-GlcNAc protein $\alpha$-crystallin, an eye lens protein consisting of two chains (A and B). The results of the relative quantification are summarized in Table I. Eight BiCy-tagged peptides were detected. Six of them showed averaged L/H ratios of 0.97 ± 0.06 to 1.09 ± 0.05 corresponding to an unspecific labeling of serine residues. For the two BiCy-tagged peptides $^{158}AIPV_{BiCy}\mathbf{S}SR^{163}$ and $^{158}AIPV_{BiCy}\mathbf{S}SREEKPSSAPSS^{173}$ of chain A, averaged L/H ratios of 2.94 ± 0.97 and 3.18 ± 0.10 were detected, which indicate a specific tagging.

To exclude false positives caused by overlapping signals and to increase the confidence of the relative quantification, we performed experiments in which labels were switched: the glycosylated sample was tagged with BiCy-d4, and the deglycosylated sample was tagged with BiCy-d0. The resulting averaged H/L ratios of 2.08 ± 0.08 and 6.17 ± 0.45 confirm the specificity of BiCy tagging of the *O*-GlcNAc peptides. The averaged H/L ratios of the unspecific peptides were 0.79 ± 0.08 to 1.03 ± 0.01. The *O*-GlcNAc site was localized on $Ser^{162}$ (supplemental Fig. 4).

*Identification of O-GlcNAcylated Peptides from Murine 20 S Proteasomes and Hsp90*—The enrichment strategy described above was applied to the analysis of 20 S protea-

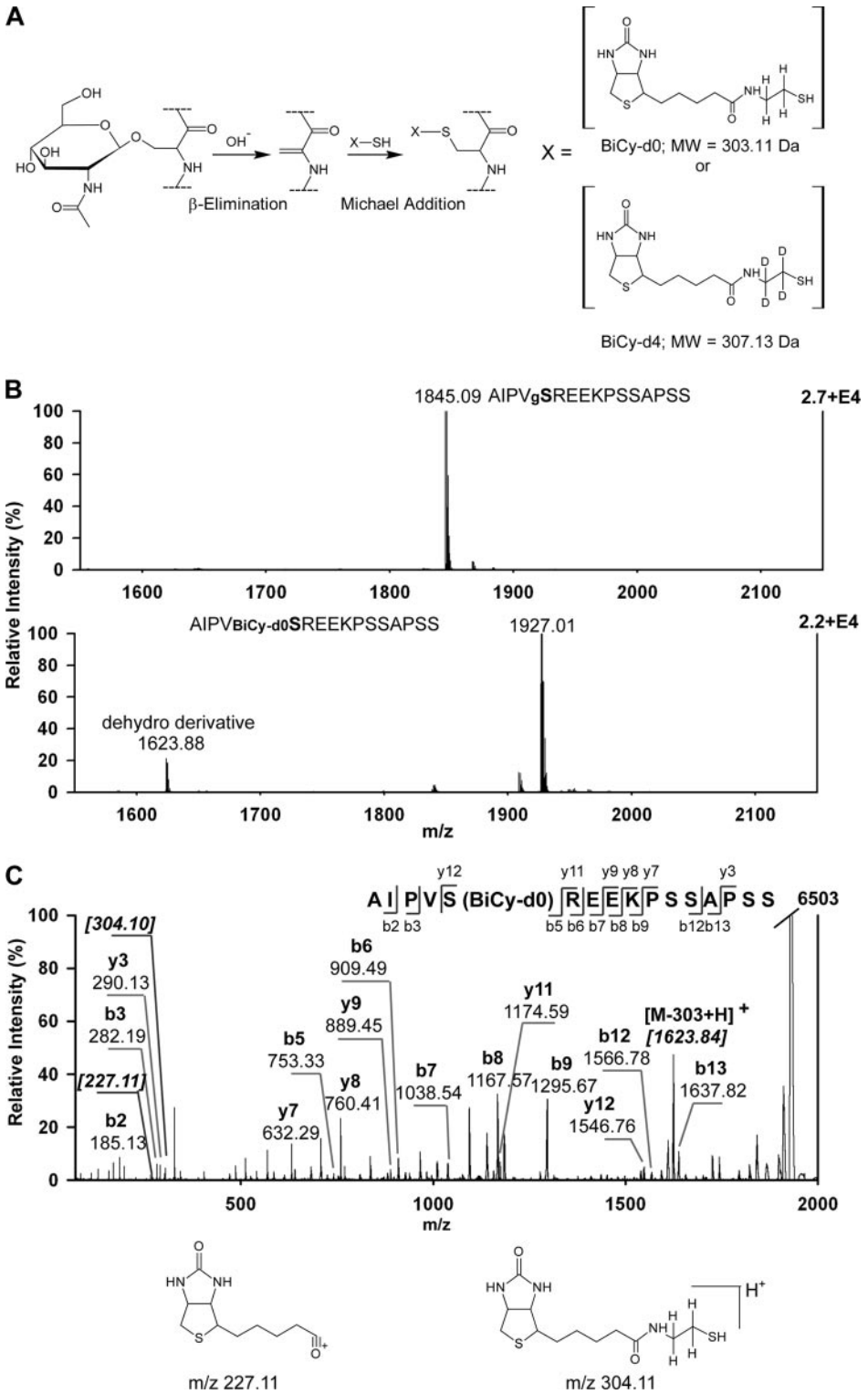


FIG. 3. **Derivatization of a synthetic *O*-GlcNAc-modified peptide by alkali-mediated β-elimination and Michael addition with a novel biotin-cystamine tag.** *A*, shown is the strategy for replacement of the *O*-GlcNAc moiety on serine or threonine residues by the stable affinity tag BiCy. To discriminate between specific and unspecific reactions, differential isotopic tags (BiCy-d0 and BiCy-d4) were synthesized. *B*, MALDI-TOF/TOF-MS spectra of a synthetic *O*-GlcNAc-modified peptide before (*upper lane*) and after derivatization with BiCy-d0 (*lower lane*). The mass shift of 82 Da corresponds to the loss of *O*-GlcNAc (−203 Da) and water (−18 Da) and the addition of BiCy-d0 (303 Da). *C*, the MALDI-TOF/TOF-MS/MS spectrum of the BiCy-tagged *O*-GlcNAc peptide with precursor mass *m/z* 1927.0 is shown. Diagnostic ions at *m/z* 227.1 and 304.1 and the neutral loss of $[M\text{-}303+H]^+$ confirm the tagging of the peptide. The site of modification is localized to Ser[5].

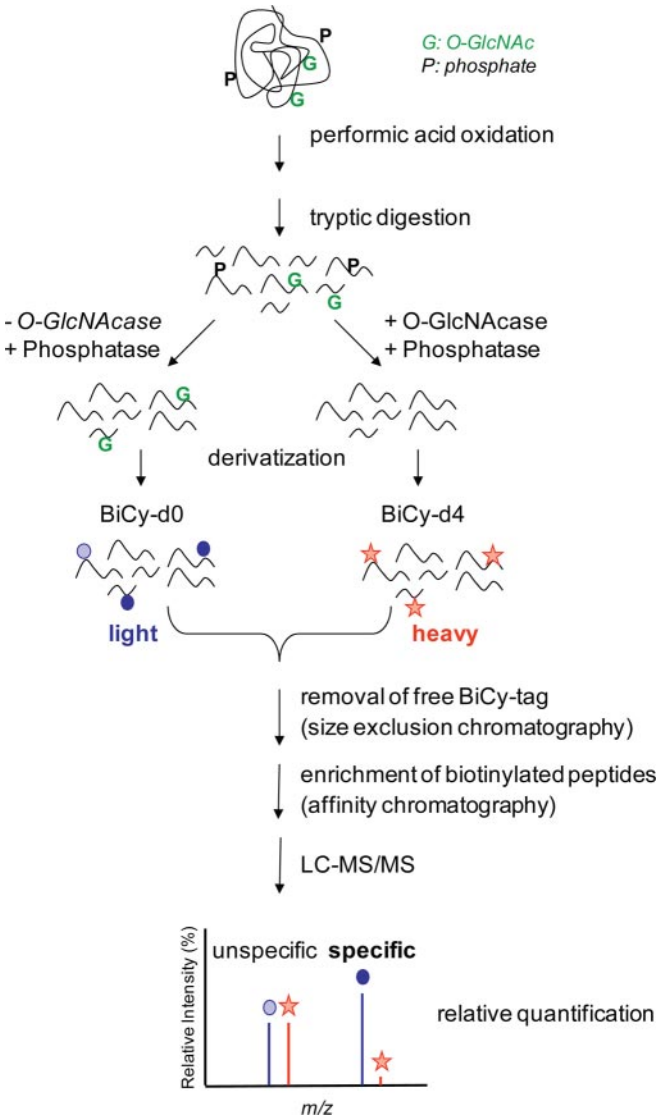


FIG. 4. **Strategy for identifying *O*-GlcNAc sites by chemical tagging with the biotin-cystamine tag BiCy and relative quantification.**

somes, as a complex biological sample, and to Hsp90, a molecular chaperone protein separated during proteasome purification. To investigate tissue-specific differences of *O*-GlcNAcylation, we analyzed proteasomes from mouse spleen (mainly comprising immunoproteasomes) and brain (mainly comprising standard proteasomes). As summarized in Table II, we identified 17 BiCy-labeled peptides with L/H (or H/L) ratios of 0.71 to greater than 10. To define the cut-off for a specific labeling, we took the L/H (and H/L) ratios of seven technical replicates from the expected 1:1 BiCy-labeled peptides of $\alpha$-crystallin and compared them in a *t* test with the ratios of the individual peptides of spleen proteasome measured in three replicates. A significance of $p < 0.001$ was found for a ratio of 1.3 (1:0.77), which corresponds to a 23% decreased intensity of the BiCy-d4-labeled peptide compared with the d0-labeled (for L/H ratios). Because the greatest deviation from the expected 1:1 ratio for $\alpha$-crystallin was 29% (ratio 0.71), we increased for more confidence the cut-off ratio to 1.43 (1:0.7), which corresponds to a reduced signal intensity of the heavy peptide of >30%. With this cut-off, we identified six proteasomal *O*-GlcNAc sites with L/H (or H/L) ratios of 1.5 to greater than 10 (Table II). In contrast, unspecific derivatization products occurred with ratios of 0.71–1.33. Representative mass spectra of specific and unspecific products are shown in Fig. 5. Remarkably, among the unspecific labeled peptides, cysteine-labeled products were also observed. N-terminal to these residues, acidic amino acids (Glu and Asp) are localized. We suppose that these residues interfere with the cysteine oxidation resulting in BiCy tagging.

A variety of the BiCy-labeled peptides (Table II) show low Mascot scores with *p* values > 0.05. Most of the labeled peptides are quite short (7–9 amino acids), and two peptides are semitryptic. Such peptides are mostly underscored in the automatic database search process (37). The appearance of semitryptic or nontryptic peptides is not unusual for digests of 20 S proteasomes. We often observed autoproteolytic products of this multiprotease complex. Furthermore, nontryptic peptides are found in every tryptic digest as proteolytic background (37). To prove the identity of the specific BiCy-labeled peptides, we synthesized analogs with a phosphate group at the detected *O*-GlcNAc site and derivatized them with BiCy-d0. We used their MS/MS spectra to compare the fragmentation pattern with the identified *O*-GlcNAc peptides (supplemental Fig. 5). In all cases we found a high congruence.

The identified five novel and one known *O*-GlcNAc-sites of the 20 S proteasome are localized on the four $\alpha$-subunits $\alpha$1 ($Ser^{5}$), $\alpha$4 ($Ser^{130}$), $\alpha$5 ($Ser^{198}$), and $\alpha$6 ($Ser^{110}$) and the $\beta$-subunit $\beta$6 ($Ser^{57}$ and $Ser^{208}$). Interestingly, only three of the six sites were modified in both analyzed tissues providing first evidence for a tissue specific differential *O*-GlcNAc modification of 20 S proteasomes. Thus modification of $\alpha$1 and $\alpha$5 were only detected in spleen (immuno) proteasomes, whereas $Ser^{208}$ glycosylation of $\beta$6 was found only in brain proteasomes. The relative quantification of enriched BiCy-tagged peptides from murine Hsp90 (liver) resulted in the identification of two novel *O*-GlcNAc sites: $Ser^{434}$ of Hsp90$\beta$ and $Ser^{461}$ of Hsp90$\alpha$/$Ser^{452}$ of Hsp90$\beta$ (Table III, MS/MS spectra, and supplemental Fig. 6). $Ser^{452}$ (Hsp90$\beta$) is also a known phosphorylation site (38). Both sites are located in the M-segment of Hsp90 thought to be essential for client protein binding, suggesting that *O*-GlcNAc modification on $Ser^{452}$ may have an opposing effect on phosphorylation-controlled Hsp90 function.

## DISCUSSION

Recent studies have shown that several subunits of the 26 S proteasome are modified by the monosaccharide GlcNAc (17–19, 25, 39). However, the individual sites of the *O*-GlcNAc modifications are unknown except for one described on sub-

TABLE I

*Relative quantification of BiCy-d0/d4-labeled peptides of bovine α-crystallin*

Peptides derived from a tryptic digestion of α-crystallin were BiCy-labeled, enriched on streptavidin beads, analyzed by MALDI-TOF/TOF mass spectrometry, and relatively quantified. Bold characters indicate a specific tagging. $_{pyr}$Q, pyroglutamat.

| Protein | Accession number[a] | Sequence | $[M + H]^+_{cal}$ | Mascot score[b] | *p* value | L/H ratio[c] | H/L ratio (label exchange)[d] | *O*-GlcNAc site |
|---|---|---|---|---|---|---|---|---|
| **Chain** A | P02470 | $^{13}$TLGPFYP$_{BiCy}$SR$^{21}$ | 1322.65 | 44 | 3.80E-05 | 1.09 ± 0.05 | 1.03 ± 0.01 | |
| | | $^{50}$$_{pyr}$Q$_{BiCy}$SLFR$^{54}$ | 918.44 | 19 | 1.20E-02 | 0.99 ± 0.05 | 0.82 ± 0.05 | |
| | | $^{55}$TVLD$_{BiCy}$SGISEVR$^{65}$ | 1460.73 | 80 | 1.20E-08 | 0.97 ± 0.03 | 0.90 ± 0.02 | |
| | | $^{104}$$_{pyr}$QDDHGYI$_{BiCy}$SR$^{112}$ | 1358.57 | 55 | 3.00E-06 | 0.97 ± 0.06 | 0.96 ± 0.06 | |
| | | $^{158}$AIPV$_{BiCy}$**S**R$^{163}$ | 927.50 | 25 | 3.20E-03 | **2.94 ± 0.97** | **2.08 ± 0.08** | **Ser$^{162}$** |
| | | $^{158}$AIPV$_{BiCy}$**S**REEKPSSAPSS$^{173}$ | 1926.95 | 26 | 2.40E-03 | **3.18 ± 0.10** | **6.17 ± 0.45** | **Ser$^{162}$** |
| | | $^{164}$EEKPS$_{BiCy}$SAPSS$^{173}$ | 1303.57 | 22 | 7.40E-03 | 1.07 ± 0.05 | 0.79 ± 0.08 | |
| Chain B | P02510 | $^{150}$KQA$_{BiCy}$SGPER$^{157}$ | 1157.57 | 37 | 2.00E-04 | 1.08 ± 0.05 | 0.97 ± 0.05 | |

[a] UniProtKB.
[b] Highest score from seven experiments; all peptides are rank 1 hits.
[c] Four technical replicates.
[d] Three technical replicates.

TABLE II

*Identified O-GlcNAc sites of murine 20 S proteasomes from spleen and brain*

Proteasomes were enzymatically digested. The resulting peptides were BiCy-labeled, enriched on streptavidin beads, analyzed by LC-MALDI-TOF/TOF MS, and relatively quantified. $_{pyr}$Q, pyroglutamat; $_{2Ox}$M, oxidized methionine. The identity of *O*-GlcNAc modified peptides (bold) was confirmed by comparison of their MS/MS spectra with the fragmentation pattern of synthetic analogs (supplemental Fig. 5).

| Subunit | Accession number[a] | Sequence | $[M + H]^+_{cal}$ | Mascot score[b] | *p* value | Spleen | | Brain L/H ratio | *O*-GlcNAc site |
|---|---|---|---|---|---|---|---|---|---|
| | | | | | | L/H ratio[c] | H/L ratio (label exchange) | | |
| **α1** | Q9QUM9 | $^{4}$G $_{BiCy}$**S**SAGFDR$^{11}$ | 1081.46 | 29 | 0.05 | **1.73 ± 0.16** | **1.53** | 1.03 | **Ser$^{5}$** |
| | | $^{31}$AINQGGLT $_{BiCy}$SVAVR$^{43}$ | 1570.81 | 46 | 6.3E-04 | 1.08 ± 0.03 | 1.07 | 0.75 | |
| **α4** | Q9Z2U0 | $^{29}$G$_{BiCy}$STAVGVR$^{36}$ | 1031.52 | 30 | 0.053 | 1.00 ± 0.01 | 0.98 | 0.86 | |
| | | $^{89}$VE$_{BiCy}$CQSHR$^{95}$ | 1127.52 | 31 | 0.024 | 1.33 ± 0.03 | 0.80 | 0.83 | |
| | | $^{125}$RPFGI$_{BiCy}$**S**AL$^{132}$ | 1145.60 | 20 | 6.9[d] | **3.51 ± 0.19** | **2.52** | **2.10** | **Ser$^{130}$** |
| **α5** | Q9Z2U1 | $^{197}$S$_{BiCy}$**S**LIILK$^{203}$ | 1058.61 | 24 | 0.11 | **2.95 ± 0.71** | 1.29 | 0.84 | **Ser$^{198e}$** |
| **α6** | Q9R1P4 | $^{90}$$_{pyr}$QE$_{BiCy}$CLDSR$^{96}$ | 1102.47 | 26 | 0.019 | 1.08 ± 0.05 | 0.71 | 0.83 | |
| | | $^{108}$LV$_{BiCy}$**S**LIGSK$^{115}$ | 1101.62 | 16 | 0.37 | **>10** | **>10** | **1.70** | **Ser$^{110}$** |
| | | $^{158}$A$_{2ox}$M$_{BiCy}$SIGAR$^{164}$ | 1022.46 | 33 | 0.025 | 1.27 ± 0.06 | 1.29 | 0.93 | |
| | | $^{209}$NV$_{BiCy}$SIGIVGK$^{217}$ | 1171.64 | 33 | 0.014 | 0.89 ± 0.16 | 0.78 | 0.87 | |
| α7 | O70435 | $^{94}$EEA$_{BiCy}$SNFR$^{100}$ | 1137.49 | 30 | 0.054 | 1.10 ± 0.17 | 0.81 | 0.93 | |
| β1i | P28076 | $^{40}$V$_{BiCy}$SAGTAVVNR$^{49}$ | 1258.65 | 66 | 1.0E-05 | 1.10 ± 0.06 | 0.91 | | |
| β2i | O35955 | $^{227}$AL$_{BiCy}$STPTEPVQR$^{237}$ | 1483.75 | 35 | 9.2E-03 | 0.97 ± 0.05 | 0.88 | | |
| β4 | Q9R1P3 | $^{87}$NLAD$_{BiCy}$CLR$^{93}$ | 1073.53 | 35 | 0.012 | 1.20 ± 0.01 | 0.95 | 0.72 | |
| **β6** | O09061 | $^{56}$L$_{BiCy}$**S**EGFSIH$^{63}$ | 1174.55 | 50 | 6.3E-03[d] | **3.69 ± 1.22** | **2.58** | **1.85** | **Ser$^{57}$** |
| | | $^{204}$DVFI$_{BiCy}$**S**AAER$^{212}$ | 1292.62 | 42 | 3.0E-03 | 1.00 ± 0.04 | 0.92 | **2.54** | **Ser$^{208}$** |
| β7 | P99026 | $^{202}$$_{pyr}$QPVL$_{BiCy}$**S**QTEAR$^{211}$ | 1396.68 | 46 | 1.3E-03 | 0.96 ± 0.01 | 0.83 | 1.04 | |

[a] UniProtKB.
[b] Highest sore from all four experiments; all peptides shown were rank 1 hits.
[c] Two technical replicates.
[d] Database searches were performed with semitrypsin as protease.
[e] Known glycosylation site (19).

unit α5 (19). Because *O*-GlcNAcylation inhibits the proteasome activity (18, 20, 40), we focused here on the mass spectrometric analysis of this modification within 20 S proteasome subunits. The main challenges in determining *O*-GlcNAc sites by mass spectrometry are the lability of the glycosidic linkage under collision-induced dissociation, as well as the low stoichiometry of this dynamic modification. Using the adapted approach that included β-elimination followed by Michael addition with dithiothreitol with a novel biotin-cystamine tag and relative quantification for specificity control of the derivatization, we were able to identify five new *O*-GlcNAc sites and confirm one previously described (19) *O*-GlcNAc site on 20 S proteasomes. Furthermore, we identified two novel modification sites on the molecular chaperone Hsp90. Our data demonstrate that the direct comparison of specific and unspecific labeled peptides by relative quantification facilitates verification of the mapped *O*-GlcNAc sites. Overall 75% of all tagged peptides were found to be unspecifically labeled with ratios of 0.71–1.33, indicating that side reactions cannot be avoided. The specifically tagged *O*-GlcNAc peptides revealed ratios of 1.53 to greater than 10. When we applied this approach to α-crystallin, we success-

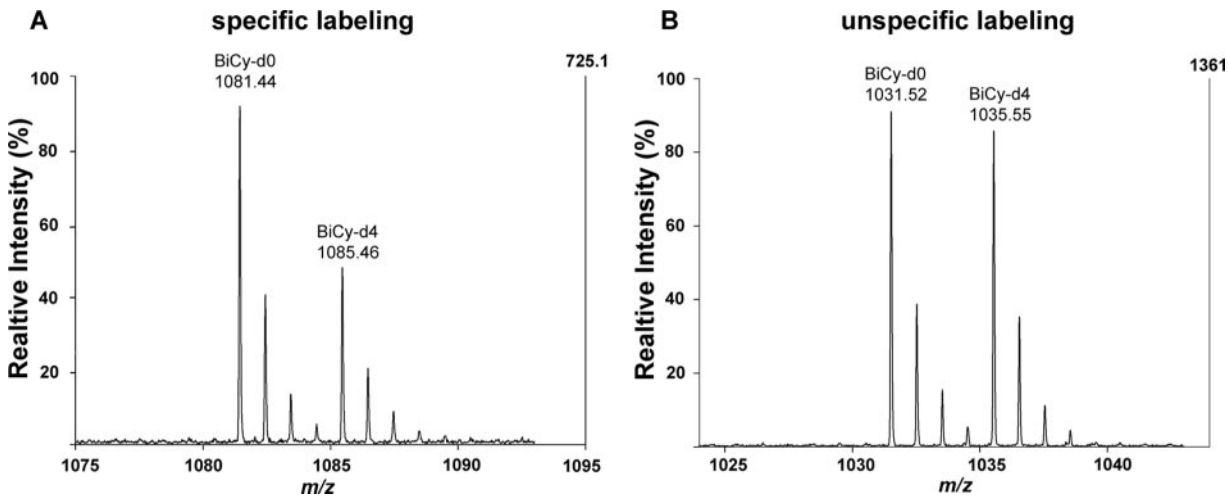


FIG. 5. **Representative mass spectra of specific and unspecific BiCy-tagged proteasomal peptides.** *A*, the isotope pattern of the peptide $^{4}G_{BiCy}$**S**SAGFDR$^{11}$ ($\alpha$1, spleen) shows an L/H ratio of ≈1.7, which indicates a specific labeling of the *O*-GlcNAcylated serine residue. *B*, a typical spectrum of an unspecific tagged peptide with a BiCy-d0/d4 ratio of 1:1 ($^{29}G_{BiCy}$STAVGVR$^{36}$, $\alpha$4 spleen) is depicted.

TABLE III

*Detection of BiCy-tagged peptides of murine HSP90 isolated from liver*

Tryptic peptides of murine Hsp90 were BiCy-labeled, enriched on streptavidin beads, analyzed by MALDI-TOF/TOF mass spectrometry, and relatively quantified. $_{pyr}$Q, pyroglutamat; $_{2Ox}$M, oxidized methionine. The identity of *O*-GlcNAc-modified peptides (bold) was confirmed by comparison of their MS/MS spectra with the fragmentation pattern of synthetic analogs (supplemental Fig. 6).

| Protein | Accession number[a] | Sequence | Mascot score[b] | *p* value | $[M + H]^{+}_{cal}$ | L/H ratio[c] | H/L ratio (label exchange)[d] | *O*-GlcNAc site |
|---|---|---|---|---|---|---|---|---|
| ***α*** | P07901 | $^{501}$DQVAN$_{BiCy}$SAFVER$^{510}$ | 78.2 | 4.2E-7 | 1520.71 | 1.01 ± 0.04 | 1.12 ± 0.03 | |
| | | $^{548}$LGIHED$_{BiCy}$SQNR$^{557}$ | 65.7 | 7.4E-7 | 1453.66 | 1.02 ± 0.03 | 1.08 ± 0.03 | |
| | | $^{587}$VVV$_{BiCy}$SNR$^{592}$ | 26.1 | 0.059 | 958.50 | 1.11 ± 0.14 | 1.05 ± 0.02 | |
| ***β*** | P11499 | $^{429}$FYEAF$_{BiCy}$**S**K$^{435}$ | 41.3 | 3.6E-3 | 1176.53 | **>10** | **>10** | **Ser$^{434}$** |
| | | $^{880}$VTI$_{BiCy}$SNR$^{885}$ | 29.1 | 0.063 | 974.50 | 1.04 ± 0.24 | 0.79 ± 0.00 | |
| ***α/β*** | P07901/P11499 | $^{460/451}$L$_{BiCy}$**S**ELLR$^{465/456}$ | 37.1 | 7.4E-3 | 1015.57 | **>10** | **>10** | **Ser$^{461}$/Ser$^{452}$** |
| | | $^{388/379}$GVVD$_{BiCy}$SEDLPLNISR$^{401/392}$ | 47.2 | 7.5E-4 | 1798.89 | 0.99 ± 0.05 | 1.05 ± 0.02 | |

[a] UniProtKB.
[b] Highest sore from all four experiments; all peptides shown were rank 1 hits.
[c] Three technical replicates.
[d] Two technical replicates.

fully detected the known *O*-GlcNAc site on Ser$^{162}$ of chain A. However, we could not identify the previously described site on Thr$^{170}$ of chain B (41). This is in accordance with the reported reduced derivatization efficiency of modified Thr residues (25) and may also explain why among all BiCy-tagged peptides of $\alpha$-crystallin, 20 S proteasomes, and Hsp90, no Thr-labeled peptides were found.

The study of 20 S proteasomes provides particular challenges. This concerns in particular the low abundance of *O*-GlcNAc modifications in connection with a very diverse 20 S proteasome population composed of several different subtypes (42). Considering that these subtypes may undergo differential post-translational modification and that *O*-GlcNAc is not a predominant modification, it appears conceivable to assume that the stoichiometry for a specific *O*-GlcNAc site within the 20 S proteasome population is extremely low. To overcome the stoichiometry problem, we employed 300 $\mu$g of purified 20 S proteasomes in each experiment. These are 150 $\mu$g of 20 S proteasome/label or 200 pmol/subunit for each of the 28 subunits (average molecular weight/subunit: 27 kDa). Assuming a stoichiometric amount of <5%, we started our analysis with ~10 pmol/modified 20 S subunit.

Our results provide the first evidence for tissue-specific differences. Specifically derivatized peptides were found for $\alpha$1 (Ser$^{5}$) and $\alpha$5 (Ser$^{198}$) only in spleen proteasomes and for $\beta$6 (Ser$^{208}$) only in brain. In contrast, the relative quantification of the *O*-GlcNAc sites of $\alpha$4 (Ser$^{130}$) and $\beta$6 (Ser$^{57}$) revealed similar L/H (H/L) ratios in both tissues. These observed variable modifications of 20 S proteasome subunits may reflect tissue-specific or even proteasome subtype-specific modification, whereby their functional implications remain to be investigated. Spleen contains predominantly 20 S immunoproteasomes, which recently were shown to play an important role in protein homeostasis and cytokine-induced oxidative stress (5). Interestingly, in rat cardiac myocytes, elevated OGT levels attenuated oxidative stress, whereas elevated OGA

levels had reciprocal effects (43). Thus elevated *O*-GlcNAc site occupancy on immunoproteasomes compared with standard proteasomes may be protective against cytokine-induced oxidative damage and/or influence their function, localization, or interaction with other proteins without the immunosubunits themselves being modified.

Interestingly, we also observed *O*-GlcNAc modifications on the molecular chaperone Hsp90 often co-purifying with 20 S proteasomes. Hsp90 induces conformational changes in client proteins (44); however, little is known about the impact of post-translational modifications on Hsp90 function. Interestingly, deletion of the yeast Ser/Thr protein phosphatase 5 that interacts with Hsp90 negatively influenced the maturation of several Hsp90 substrates (45). Because OGT binds to substrates via the same tetratricopeptide repeat motives, OGT may transiently bind to Hsp90 during *O*-GlcNAc attachment with *O*-GlcNAc modification on $Ser^{452}$ (Hsp90$\beta$) opposing phosphorylation regulated Hsp90 function. Because Hsp70 exhibits a lectinic activity toward *O*-GlcNAc (46), a reciprocal *O*-GlcNAcylation/phosphorylation might control Hsp90/Hsp70 interaction and thus influence the equilibrium between repair and proteasomal degradation of client proteins.

Therefore investigating the influence of phosphorylation/*O*-GlcNAc on the Hsp70/Hsp90 machinery in collaboration with the ubiquitin proteasome system seems to be a challenging but promising field of research. Our *O*-GlcNAc site assignments offer the opportunity for hypothesis-driven approaches to analyze the biological impact of *O*-GlcNAc on proteasomes and Hsp90.

*Acknowledgments*—We thank Matthias Selbach and Bjoern Schwanhaeusser for the performance of additional ESI-Orbitrap MS measurements; Ilse Drung, Barbara Brecht, and Prisca Kunert for technical assistance; Michele Mishto and Andrean Goede for statistical calculations; and Burkhardt Dahlmann for helpful comments and critical reading of the manuscript.

* This work was supported by Deutsche Forschungsgemeinschaft Grants SFB 421 and KL427/15-1 (to P. M. K. L.) and in part by Sonnenfeldstiftung Grant XII/206 (to T. O.).

[S] This article contains supplemental material.

** To whom correspondence should be addressed. Tel.: 49-30-450-528-142; Fax: 49-30-450-528-921; E-mail: p-m.kloetzel@charite.de.

REFERENCES

1. Rock, K. L., Gramm, C., Rothstein, L., Clark, K., Stein, R., Dick, L., Hwang, D., and Goldberg, A. L. (1994) Inhibitors of the proteasome block the degradation of most cell proteins and the generation of peptides presented on MHC class I molecules. *Cell* **78,** 761–771
2. Coux, O., Tanaka, K., and Goldberg, A. L. (1996) Structure and functions of the 20S and 26S proteasomes. *Annu. Rev. Biochem.* **65,** 801-847
3. Kloetzel, P. M. (2001) Antigen processing by the proteasome. *Nat. Rev. Mol. Cell Biol.* **2,** 179–187
4. Rock, K. L., York, I. A., Saric, T., and Goldberg, A. L. (2002) Protein degradation and the generation of MHC class I-presented peptides. *Adv. Immunol.* **80,** 1–70
5. Seifert, U., Bialy, L. P., Ebstein, F., Bech-Otschir, D., Voigt, A., Schröter, F., Prozorovski, T., Lange, N., Steffen, J., Rieger, M., Kuckelkorn, U., Aktas, O., Kloetzel, P. M., and Krüger, E. (2010) Immunoproteasomes preserve protein homeostasis upon interferon-induced oxidative stress. *Cell* **142,** 613–624
6. Bose, S., Stratford, F. L., Broadfoot, K. I., Mason, G. G., and Rivett, A. J. (2004) Phosphorylation of 20S proteasome $\alpha$ subunit C8 (alpha7) stabilizes the 26S proteasome and plays a role in the regulation of proteasome complexes by $\gamma$-interferon. *Biochem. J.* **378,** 177–184
7. Liu, X., Huang, W., Li, C., Li, P., Yuan, J., Li, X., Qiu, X. B., Ma, Q., and Cao, C. (2006) Interaction between c-Abl and Arg tyrosine kinases and proteasome subunit PSMA7 regulates proteasome degradation. *Mol. Cell* **22,** 317–327
8. Zong, C., Gomes, A. V., Drews, O., Li, X., Young, G. W., Berhane, B., Qiao, X., French, S. W., Bardag-Gorce, F., and Ping, P. (2006) Regulation of murine cardiac 20S proteasomes: Role of associating partners. *Circ. Res.* **99,** 372–380
9. Zhang, F., Paterson, A. J., Huang, P., Wang, K., and Kudlow, J. E. (2007) Metabolic control of proteasome function. *Physiology* **22,** 373–379
10. Haass, C., and Kloetzel, P. M. (1989) The *Drosophila* proteasome undergoes changes in its subunit pattern during development. *Exp. Cell Res.* **180,** 243–252
11. Castaño, J. G., Mahillo, E., Arizti, P., and Arribas, J. (1996) Phosphorylation of C8 and C9 subunits of the multicatalytic proteinase by casein kinase II and identification of the C8 phosphorylation sites by direct mutagenesis. *Biochemistry* **35,** 3782–3789
12. Lu, H., Zong, C., Wang, Y., Young, G. W., Deng, N., Souda, P., Li, X., Whitelegge, J., Drews, O., Yang, P. Y., and Ping, P. (2008) Revealing the dynamics of the 20 S proteasome phosphoproteome: A combined CID and electron transfer dissociation approach. *Mol. Cell. Proteomics* **7,** 2073–2089
13. Tokunaga, F., Aruga, R., Iwanaga, S., Tanaka, K., Ichihara, A., Takao, T., and Shimonishi, Y. (1990) The $NH_2$-terminal residues of rat liver proteasome (multicatalytic proteinase complex) subunits, C2, C3 and C8, are $N^{\alpha}$-acetylated. *FEBS Lett.* **263,** 373–375
14. Lilley, K. S., Davison, M. D., and Rivett, A. J. (1990) N-terminal sequence similarities between components of the multicatalytic proteinase complex. *FEBS Lett.* **262,** 327–329
15. Kimura, Y., Takaoka, M., Tanaka, S., Sassa, H., Tanaka, K., Polevoda, B., Sherman, F., and Hirano, H. (2000) $N^{\alpha}$-acetylation and proteolytic activity of the yeast 20 S proteasome. *J. Biol. Chem.* **275,** 4635–4639
16. Wang, X., Chen, C. F., Baker, P. R., Chen, P. L., Kaiser, P., and Huang, L. (2007) Mass spectrometric characterization of the affinity-purified human 26S proteasome complex. *Biochemistry* **46,** 3553–3565
17. Sümegi, M., Hunyadi-Gulyás, E., Medzihradszky, K. F., and Udvardy, A. (2003) 26S proteasome subunits are *O*-linked *N*-acetylglucosamine-modified in *Drosophila melanogaster*. *Biochem. Biophys. Res. Commun.* **312,** 1284–1289
18. Zhang, F., Su, K., Yang, X., Bowe, D. B., Paterson, A. J., and Kudlow, J. E. (2003) *O*-GlcNAc modification is an endogenous inhibitor of the proteasome. *Cell* **115,** 715–725
19. Wang, Z., Park, K., Comer, F., Hsieh-Wilson, L. C., Saudek, C. D., and Hart, G. W. (2009) Site-specific GlcNAcylation of human erythrocyte proteins: Potential biomarker 19 (s) for diabetes. *Diabetes* **58,** 309–317
20. Zhang, F., Hu, Y., Huang, P., Toleman, C. A., Paterson, A. J., and Kudlow, J. E. (2007) Proteasome function is regulated by cyclic AMP-dependent protein kinase through phosphorylation of Rpt6. *J. Biol. Chem.* **282,** 22460–22471
21. Keembiyehetty, C. N., Krzeslak, A., Love, D. C., and Hanover, J. A. (2011) A lipid-droplet-targeted *O*-GlcNAcase isoform is a key regulator of the proteasome. *J. Cell Sci.* **124,** 2851–2860
22. Hart, G. W., Slawson, C., Ramirez-Correa, G., and Lagerlof, O. (2011) Cross talk between *O*-GlcNAcylation and phosphorylation: Roles in signaling, transcription, and chronic disease. *Annu. Rev. Biochem.* **80,** 825–858
23. Liu, F., Iqbal, K., Grundke-Iqbal, I., Hart, G. W., and Gong, C. X. (2004) *O*-GlcNAcylation regulates phosphorylation of tau: A mechanism involved in Alzheimer's disease. *Proc. Natl. Acad. Sci. U.S.A.* **101,** 10804–10809
24. Vosseller, K., Trinidad, J. C., Chalkley, R. J., Specht, C. G., Thalhammer, A., Lynn, A. J., Snedecor, J. O., Guan, S., Medzihradszky, K. F., Maltby, D. A., Schoepfer, R., and Burlingame, A. L. (2006) *O*-Linked *N*-acetylglucosamine proteomics of postsynaptic density preparations using lectin weak affinity chromatography and mass spectrometry. *Mol. Cell. Proteomics* **5,** 923–934

25. Wells, L., Vosseller, K., Cole, R. N., Cronshaw, J. M., Matunis, M. J., and Hart, G. W. (2002) Mapping sites of *O*-GlcNAc modification using affinity tags for serine and threonine post-translational modifications. *Mol. Cell. Proteomics* **1,** 791–804
26. Khidekel, N., Arndt, S., Lamarre-Vincent, N., Lippert, A., Poulin-Kerstien, K. G., Ramakrishnan, B., Qasba, P. K., and Hsieh-Wilson, L. C. (2003) A chemoenzymatic approach toward the rapid and sensitive detection of *O*-GlcNAc posttranslational modifications. *J. Am. Chem. Soc.* **125,** 16162–16163
27. Wang, Z., Udeshi, N. D., O'Malley, M., Shabanowitz, J., Hunt, D. F., and Hart, G. W. (2010) Enrichment and site mapping of *O*-linked *N*-acetylglucosamine by a combination of chemical/enzymatic tagging, photochemical cleavage, and electron transfer dissociation mass spectrometry. *Mol. Cell. Proteomics* **9,** 153–160
28. Parker, B. L., Gupta, P., Cordwell, S. J., Larsen, M. R., and Palmisano, G. (2011) Purification and identification of *O*-GlcNAc-modified peptides using phosphate-based alkyne CLICK chemistry in combination with titanium dioxide chromatography and mass spectrometry. *J. Proteome Res.* **10,** 1449–1458
29. Klement, E., Lipinszki, Z., Kupihár, Z., Udvardy, A., and Medzihradszky, K. F. (2010) Enrichment of *O*-GlcNAc modified proteins by the periodate oxidation-hydrazide resin capture approach. *J. Proteome Res.* **9,** 2200–2206
30. Vosseller, K., Hansen, K. C., Chalkley, R. J., Trinidad, J. C., Wells, L., Hart, G. W., and Burlingame, A. L. (2005) Quantitative analysis of both protein expression and serine/threonine post-translational modifications through stable isotope labeling with dithiothreitol. *Proteomics* **5,** 388–398
31. Dahlmann, B., Ruppert, T., Kuehn, L., Merforth, S., and Kloetzel, P. M. (2000) Different proteasome subtypes in a single tissue exhibit different enzymatic properties. *J. Mol. Biol.* **303,** 643–653
32. Kuckelkorn, U., Ruppert, T., Strehl, B., Jungblut, P. R., Zimny-Arndt, U., Lamer, S., Prinz, I., Drung, I., Kloetzel, P. M., Kaufmann, S. H., and Steinhoff, U. (2002) Link between organ-specific antigen processing by 20S proteasomes and CD8(+) T cell-mediated autoimmunity. *J. Exp. Med.* **195,** 983–990
33. McLachlin, D. T., and Chait, B. T. (2003) Improved $\beta$-elimination-based affinity purification strategy for enrichment of phosphopeptides. *Anal. Chem.* **75,** 6826–6836
34. Girault, S., Chassaing, G., Blais, J. C., Brunot, A., and Bolbach, G. (1996) Coupling of MALDI-TOF mass analysis to the separation of biotinylated peptides by magnetic streptavidin beads. *Anal. Chem.* **68,** 2122–2126
35. Li, W., Backlund, P. S., Boykins, R. A., Wang, G., and Chen, H. C. (2003) Susceptibility of the hydroxyl groups in serine and threonine to $\beta$-elimination/Michael addition under commonly used moderately high-temperature conditions. *Anal. Biochem.* **323,** 94–102
36. Borisov, O. V., Goshe, M. B., Conrads, T. P., Rakov, V. S., Veenstra, T. D., and Smith, R. D. (2002) Low-energy collision-induced dissociation fragmentation analysis of cysteinyl-modified peptides. *Anal. Chem.* **74,** 2284–2292
37. Picotti, P., Aebersold, R., and Domon, B. (2007) The implications of proteolytic background for shotgun proteomics. *Mol. Cell. Proteomics* **6,** 1589–1598
38. Dephoure, N., Zhou, C., Villén, J., Beausoleil, S. A., Bakalarski, C. E., Elledge, S. J., and Gygi, S. P. (2008) A quantitative atlas of mitotic phosphorylation. *Proc. Natl. Acad. Sci. U.S.A.* **105,** 10762–10767
39. Sprung, R., Nandi, A., Chen, Y., Kim, S. C., Barma, D., Falck, J. R., and Zhao, Y. (2005) Tagging-via-substrate strategy for probing *O*-GlcNAc modified proteins. *J. Proteome Res.* **4,** 950–957
40. Liu, K., Paterson, A. J., Zhang, F., McAndrew, J., Fukuchi, K., Wyss, J. M., Peng, L., Hu, Y., and Kudlow, J. E. (2004) Accumulation of protein *O*-GlcNAc modification inhibits proteasomes in the brain and coincides with neuronal apoptosis in brain areas with high *O*-GlcNAc metabolism. *J. Neurochem.* **89,** 1044–1055
41. Roquemore, E. P., Chevrier, M. R., Cotter, R. J., and Hart, G. W. (1996) Dynamic *O*-GlcNAcylation of the small heat shock protein $\alpha$B-crystallin. *Biochemistry* **35,** 3578–3586
42. Kloss, A., Meiners, S., Ludwig, A., and Dahlmann, B. (2010) Multiple cardiac proteasome subtypes differ in their susceptibility to proteasome inhibitors. *Cardiovasc. Res.* **85,** 367–375
43. Ngoh, G. A., Watson, L. J., Facundo, H. T., and Jones, S. P. (2011) Augmented *O*-GlcNAc signaling attenuates oxidative stress and calcium overload in cardiomyocytes. *Amino Acids* **40,** 895–911
44. Wandinger, S. K., Richter, K., and Buchner, J. (2008) The Hsp90 chaperone machinery. *J. Biol. Chem.* **283,** 18473–18477
45. Wandinger, S. K., Suhre, M. H., Wegele, H., and Buchner, J. (2006) The phosphatase Ppt1 is a dedicated regulator of the molecular chaperone Hsp90. *EMBO J.* **25,** 367–376
46. Guinez, C., Lemoine, J., Michalski, J. C., and Lefebvre, T. (2004) 70-kDa-heat shock protein presents an adjustable lectinic activity toward *O*-linked *N*-acetylglucosamine. *Biochem. Biophys. Res. Commun.* **319,** 21–26